Proceedings of the 10th World Congress on Momentum, Heat and Mass Transfer (MHMT 2025)
Barcelona, Spain - April, 2025
Paper No. ENFHT 138
DOI: 10.11159/enfht25.138

Strategies for Hybrid Immersion Cooling Of Light Electric Vehicle Battery Packs: A Numerical Investigation

Stefano Landini[1], Jack Panter[1], Anindita Roy[2], Gordhan Das Valasai[3], Mohammad Fawzi Ismail[4]
[1]School of Engineering, Mathematics and Physics, University of East Anglia, NR4 7TJ, Norwich UK
s.landini@uea.ac.uk; j.panter@uea.ac.uk
[2]Mechanical Engineering Department, Symbiosis Institute of Technology, Symbiosis International (Deemed) University, Pune 412115, India
anindita.roy@sitpune.edu.in
[3] Department of Mechanical Engineering, Quaid -e- Awam University of Engineering, Science and Technology, Sakrand Road, Nawabshah, Shaheed Benazirabad, Sindh 67450, Pakistan
valasai@quest.edu.pk
[4] Department of Renewable Energy Engineering, Amman Arab University, Amman, Jordan
m.ismail@aau.edu.jo

Abstract – This work investigates a new hybrid thermal management system (TMS) for light electric vehicle (LEV) battery packs that uses dielectric liquid immersion cooling and heat pipes to effectively control lithium-ion battery (LIB) thermal load. The proposed TMS exploits the heat pipes' excellent heat dissipation and dielectric fluids' uniform cooling. Different commercial dielectric oil chemistries (Cargill DE-11772 and EF-3221, LK-STO50, and MIVOLT-DFK) are evaluated as heat transfer fluids (HTFs) and compared with air and deionised water as benchmark. A 3D steady-state CFD model is developed in Ansys 2024R1 to simulate the proposed TMS for a 4S4P (14.8V, 10 Ah) Lithium-Nickel Manganese Cobalt (NMC) battery pack. Under typical 2C discharge rate, the model preliminarily examines the TMS thermal performance when simulating heat transfer with and without buoyancy effects. Buoyancy improves cooling performance, especially for viscous fluids, lowering battery, HTF, and heat sink temperatures by 20%. With modest LIB heat generation rates (up to 25 kW/m³), the TMS ensures effective cooling with minimum temperature increase. However, when reaching heat generation rates up to 100 kW/m³, the battery temperature reaches 91.13°C, revealing the system's cooling capability limitations. The study examines the effect of changing heat sink and insulation equivalent convective heat transfer coefficients. Increasing the heat sink coefficient from 10 to 100 W/m²K lowers the battery temperature from 138°C to 49°C, while increasing the insulation equivalent heat transfer coefficient from 1 to 50 W/m²K lowers battery temperature from 92°C to 46°C. This study shows that the hybrid TMS using heat pipes and immersion cooling may improve compact LEV safety, performance, and battery longevity under high-demand situations.

***Keywords*:** Lithium-Ion Batteries, Light Electric Vehicles, Thermal Management, Immersion Cooling, Dielectric Oils, Heat Pipes, Passive Cooling

Nomenclature

TMS	Thermal management system	$\dot{q}_{cell}$	volumetric heat generation rate
LEV	light electric vehicle	k_{cell}	thermal conductivity
LIB	lithium-ion battery	ρ	Density (kg/m^3)
CFD	Computational fluid dynamic	Cp	Specific heat (J/kg k)
LIBs	Lithium-ion batteries	k	Thermal conductivity (W/m K)
DR	Discharge rates	μ	Viscosity (Pa s)
NCM	Nickel Cobalt Manganese	β	Thermal expansion coefficient (1/K)
HTF	heat transfer fluid	T	Temperature
LSBC	Least Squared Cell Based	b	Battery
		htf	Heat transfer fluid
		sink	Sink

1. Introduction

Lithium-ion batteries (LIBs) power electric vehicles (EVs) due to their high energy storage capacity, low mass, and extended lifespan. The efficiency and safety of such devices are susceptible to temperature changes. Thermal runaway occurs when the battery temperature rises uncontrolled, posing a danger of fire or explosion that can only be prevented by a thermal management system (TMS). Due to high discharge rates (DR) and battery pack conditions, including high heat, EVs and other high-power applications have that problem. Besides being safe, the components are properly shielded, and the battery lasts longer and performs better [1, 2].

Since LIBs are widely utilised in EVs, innovative cooling techniques for thermal load management have been extensively studied. Though inefficient at high power utilisation, conventional air-cooling solutions are more popular due to their simplicity. Specifically in two-wheeled EVs, the space available for an intricate cooling mechanism is insufficient, therefore effective compact light TMS are needed. Researchers have developed PCMs, passive and active liquid cooling, and hybrid cooling methods to address these issues. Fluid chemistry, flow rate, ambient temperature, and battery configuration affect fluid efficacy and cooling performance. By optimising battery pack temperature and eliminating thermal gradients, a well-designed TMS may improve LIB safety, performance, and lifespan [3, 4].

Air cooling is one of the simplest and most affordable ways for controlling LIB temperature. It broadly consists in blowing air across the battery cells to remove the generate heat during operation. Misar and Thombre [5] analysed the application of high-thermal-conductivity potting material along with air cooling to a 3S3P NMC 21700 battery pack in electric two-wheelers. This configuration was discovered to lower temperature variation by a quarter, enhancing temperature uniformity within the battery pack. In a similar manner, Zhang, et al. [6] also worked on airflow control in an air cooled LIB pack observing that altering the position of the air cooling channel exit led to reduced maximum figure of temperature and thermal non-uniformity with improvement under 2C discharge rates.

Liquid cooling systems use a coolant, e.g. mixture of water or water glycol, which flows through conduits interior or exterior of the battery pack to remove heat. Suresh Patil, et al. [7] compared water-glycol cold plate cooling with dielectric fluid immersion cooling of a 50 V LIB pack. This proved that the immersion cooling system was capable to reduce the maximum temperature by 9.3% during high discharge rates (up to 5C) more than the water-glycol cooling technique. Additionally, Wu, et al. [8] also pointed other modern challenges noting that higher flow rates of coolants results in excessive energy consumption without a proportional improvement of cooling. Nonetheless, Wu, et al. [8], and Liu, et al. [9] highlighted that the water-glycol mixtures and other liquid coolants can deliver lower maximum temperature in high-rate discharge.

Immersion cooling consists in the entire battery pack being submerged in a dielectric (non-electrically conductive) fluid which absorbs heat and dissipates it by natural buoyancy-driven convection cells into a heat sink. This method is particularly effective to avoid concentration of heat (thermal hotspots) and cool all the surface of the battery uniformly including the tabs, so it is suitable for high power and/or high energy density LIB. Thiru Kumaran and Hemavathi [10] proved that the maximum temperature of a 50 V LIB pack under 3C discharges could effectively drop by 35.95% if using dielectric fluid immersion cooling, thus preventing thermal runaway. Williams, et al. [11] also independently confirmed the usability of Novec 7000 dielectric fluid to keep the thermal difference to below 1°C across a 26650 $LiFePO_4$ cylindrical cell module charging at up to 4C rate. As Thiru Kumaran and Hemavathi [10] and Williams, et al. [11] stated, when mineral oil and Novec 7000 dielectric fluids were used, battery temperatures reduced, and temperature differences in the battery modules were measured minimally. Liquid dielectrics minimise electrical short circuits and offer uniform cool flow rates and heat dissipation without electric conductivity.

Novel interest in the research community is now focusing on combination of cooling systems to enhance thermal performance and reduce volumes, weight, and cost. The latter is typically achieved by constraining the TMs mechanism to be based on passive heat transfer. Zou, et al. [12] recently investigated a dual-cooling system which incorporated static liquid immersion and liquid forced convection tubes. This system was able to lower the maximum temperature of battery module to 43.3°C when discharging at a rate of 3C at an ambient temperature of 25°C. Wang, et al. [13] proved that by using both immersion and direct forced convection cooling method, safe LIB operation time below 35°C was extended by 150% compared to air natural convection. Wang, et al. [14] investigated two-phase dielectric liquid immersion cooling integrated with forced air-cooling. The hybrid system was shown to be effective in enhancing temperature uniformity under during high-rate discharges. Similarly, in Liu, et al. [15] and Zhu, et al. [16], it was demonstrated that the use of multiple cooling techniques would help to enhance the overall regulating ability and safety.

From the revised literature, there is evidence of limited research efforts on developing light compact cost-effective TMS for two-wheeled electric vehicles (EVs) and light electric vehicles (LEVs), which are gaining steeply popularity across cities in all continents, especially EU and Asia. In these applications, air-cooled systems, whether natural or induced convection, are currently adopted due to spatial constraints and the complexities associated with indirect liquid cooling systems. However, these TMS are proved to be inadequate for maintaining optimal temperature control independent of environmental conditions. Therefore, this research aims to evaluate the feasibility of a novel hybrid passive LIB TMS that integrates dielectric liquid immersion cooling with heat pipes, specifically tailored for electric two-wheeler applications. Preliminary numerical investigations were conducted on a prototype of this hybrid immersion cooling system, which operates without fluid circulation.

2. Methodology

2.1. Geometry

This study included the design and thermal performance evaluation by CFD numerical analysis of a single-phase immersion cooled battery pack equipped with heat pipes for rapid heat dissipation. A prototype (Figure 1) is based on a typical 2-wheeler 4S4P (4 series, 4 parallel) 14.8V 10 Ah Lithium-Nickel Manganese Cobalt (NMC) oxide LIB, where cylindrical cells are typically preferred being more readily available, less expensive, and easier to assemble. The properties of the NMC LIB are reported in Table 1. All numerical simulations conducted where based on a steady-state operating condition and a discharge rate of 2C. This represents a stress condition of 2-wheeler EV battery pack. A three-dimensional steady-state CFD model of the entire system, including LIB NMC cells, fins, heat pipes, heat sink, and heat transfer fluid (HTF) was created on ANSYS (2024 R1) to simulate the physics and evaluate the performance of the proposed LIB TMS. The aim was to examine the effectiveness of immersion cooling with different heat transfer fluid (HTF) chemistries and compare it with air and deionised water as the benchmark.

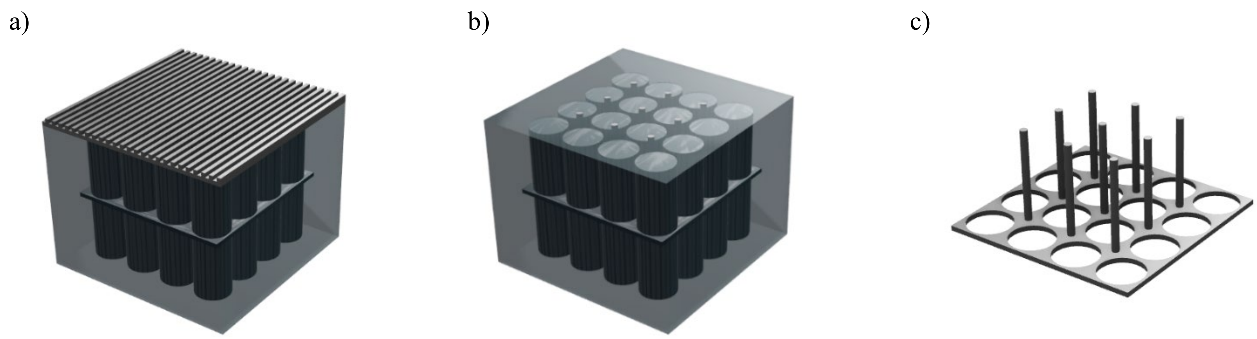

Figure 1: Hybrid thermal management system proposed including immersion single-phase liquid cooling, fin, heat pipes and heat sink: a) overall view including heat sink on top, (b) overall system excluding heat sink, c) focus on fin and 9 x heat pipes.

Table 1: Thermophysical properties of LIB NMC 18650 cells

Parameter	**Value**
Diameter [mm]	18
Height [mm]	65
Nominal capacity [Ah]	2.5
Nominal voltage [V]	3.7
Minimum/Maximum cut-off voltage [V]	2.8 / 4.8
Cathode/Anode Chemistry	NMC / Graphite
Density [kg/m3]	2,000
Specific Heat Capacity [J/kg K]	1,000
Radial Thermal Conductivity [W/m K]	1
Axial Thermal Conductivity [W/m K]	30

2.2. Computational Fluid Dynamics Modelling

All simulations were based on a constant LIB cells' volumetric heat generation rate of 100 kW/m^3 based on experimental evidenced gathered, representative of a standard 2C discharge rate for 18650 LIB NMC cells. Within the cell body, only the energy balance is solved (Equation 1), where k_{cell} stands for the effective anisotropic thermal conductivity (W/m K), and $\dot{q}_{cell}$ denotes the volumetric heat generation rate (W/m^3) of the battery. Direction determines the LIB cell's effective thermal conductivity k_{cell}, which is 1 W/m K in the radial direction and 30 W/m K in the axial direction, as reported in Table 1.

$$\dot{q}_{cell} = -\nabla \cdot (k_{cell} \nabla T) \tag{1}$$

Within the HTF body, continuity, momentum and energy equations are solved (Equation 2,3,4). A laminar viscous model was employed, as the HTF is confined withing an enclosure and no turbulence builds up. The buoyancy effect was implemented by employing a Boussinesq model for the density based on appropriate expansion coefficient (reported in Table 2). The different HTF chemistries employed included air, deionised water, and a selection of commercial dielectric oils typically employed for transformers cooling (Cargill DE11772 and EF3221, LK-STO50, MIVOLT-DFK). The HTF thermophysical properties are reported in Table 2.

The same set of equations are solved for the fin and heat pipe bodies, where $\boldsymbol{v} = 0$. Heat pipes were simulated as equivalent full metal bodies with the same thermophysical properties of the fin (Al) apart from an equivalent effective thermal conductivity (10,000 W/m K) to represent the two-phase liquid-gas phase change-based heat transfer. Both material's thermophysical properties are reported in Table 2.

$$\nabla \cdot (\rho \boldsymbol{v}) = 0 \tag{2}$$

$$\nabla \cdot (\rho \boldsymbol{v} \boldsymbol{v}) = -\nabla P + \rho \mathbf{g} + \nabla \cdot (\mu \nabla \boldsymbol{v}) \tag{3}$$

$$\nabla \cdot \left[\rho \boldsymbol{v} \left(h + \frac{v^2}{2}\right)\right] = \nabla \cdot [k \nabla T + (\mu \nabla \boldsymbol{v}) \cdot \boldsymbol{v}] \tag{4}$$

Table 2: Thermophysical properties of different HTF, fins (Al) and equivalent heat pipe solid metal

Fluid	**ρ (kg/m^3)**	**Cp (J/kg k)**	**k (W/m K)**	**μ (Pa s)**	**β (1/K)**
Air	1.225	1006	0.0242	1.799E-05	0.0034
Deionised Water	998	4182	0.6	1.003E-03	0.0002
Cargill DE-11772	860	1500	0.132	2.838E-03	0.0008
Cargill EF-3221	910	1970	0.148	7.01E-03	0.0008
LK-STO50	960	1510	0.151	5.00E-02	0.0008
MIVOLT-DFK	968	1902	0.147	7.26E-02	0.0008
Fin (Al)	2719	871	202.4	-	-
Heat Pipes	2719	871	10,000	-	-

The CFD solution method included pressure-based solver, SIMPLEC pressure-velocity coupling, Least Squared Cell Based (LSBC) gradient discretisation, PRESTO pressure spatial discretisation and second order upwind discretisation for both momentum and energy equations. All steady-state simulations were initialised at 25°C and steady fluid ($\boldsymbol{v} = 0$). The following assumptions were applied: (i) all materials properties were considered constant and equal to the average values across the expected operating temperature range; (ii) the impact of the HTF buoyancy was included by employing the Boussinesq modelling of the density and gravity equal to 9.81 m/s^2; (iii) heat transfer is in three dimensions; (iv) radiation heat transfer is negligible; (v) ideal thermal contact between all bodies, i.e. negligible thermal contact resistances; (vi) constant LIB cell heat generation rate during steady state (worst case scenario); (vii) due to the geometrical and thermal symmetry conditions, a quarter of the real control volume was simulated identifying three types of boundary conditions (i.e. walls), being symmetry, convection and insulation a shown in Figure 2; (viii) convective cooling on the heat sink based on an equivalent heat transfer coefficient of 20 W/m^2 K and 25°C, unless specified differently; (xi) insulation TMS walls characterised by an equivalent heat transfer coefficient of 1 W/m^2 K and 25°C, unless specified differently.

a) b) c)

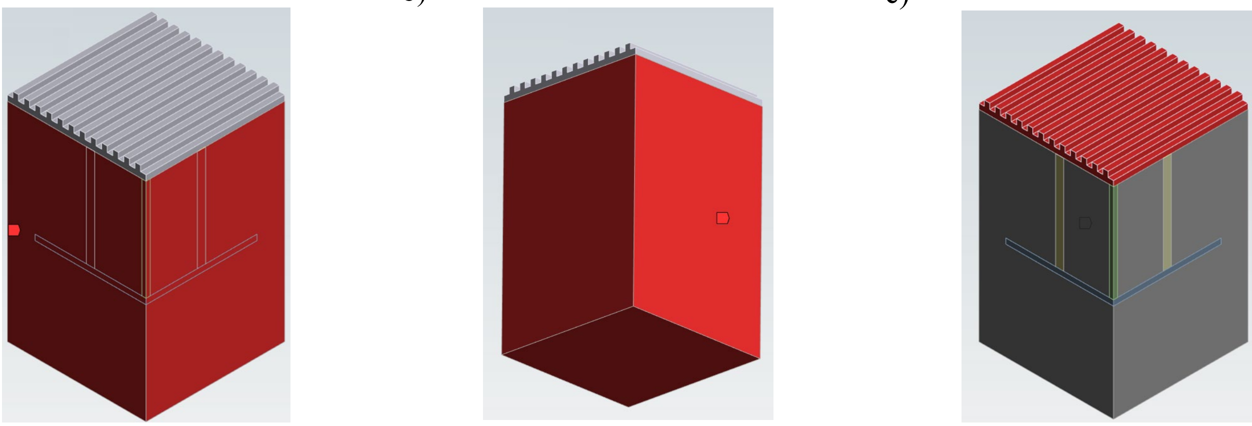

Figure 2: View of the control volume simulated in ANSYS equal to a quarter of the real TMS shown in Figure 1. The external boundary walls are clearly identified: a) symmetry wall, b) insulation wall, c) convection (heat sink) wall.

2.3. Mesh sensitivity analysis

A mesh based on shared topology between bodies was generated in Ansys Mesh. An example of a generated mesh is reported in Figure 3 for reference. A thorough mesh independency study was carried out by changing the element size in all bodies and carry on simulations for three selected HTF, being air, deionised water, and Cargill DE-11772. This was done to identify the minimum number of elements necessary to minimise solution sensitivity, processing time, and RAM.

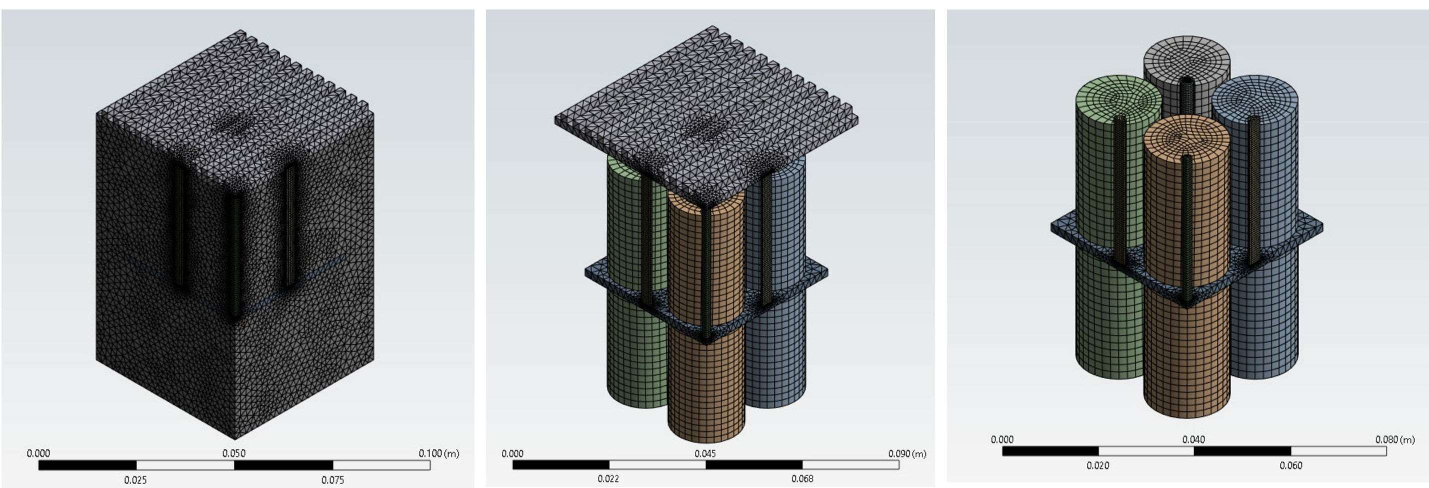

Figure 3: Example of mesh generated in ANSYS, with a specific focus on: a) overall system, b) battery cells, fin, heat pipes, heat sink, c) battery cells, fin, heat pipes.

The results of the mesh independency study are reported in Figure 4, showing the variation of temperature of battery (Tb), HTF (Thtf), and heat sink (Tsink) volume-average temperature for different mesh element counts, from course (53k elements) to fine (954k elements). It is evident that for all HTF 358k elements (green line in Figure 4) guarantee mesh independency while minimising processing time and RAM. Henceforth, this mesh was selected for all simulations.

3. Results

3.1. Effect of HTF buoyancy and chemistry

The TMS cooling effectiveness, with and without buoyancy effects, is shown in Figure 5, showing the average volume temperature for battery (Tb), HTF (Thtf) and heat sink (Tsink). In the absence of buoyancy, temperatures generally rise in all HTF owing to restricted natural convective heat transfer. For instance, buoyancy contributes to reducing the average battery temperature from 100.16°C to 91.97°C when using Cargill DE-11772. This behaviour is reflected for all HTF, an average decrease of battery temperature across different HTF of 5.32°C. These comparisons demonstrate that buoyancy improves overall cooling efficiency by promoting more efficient heat transfer, especially in fluids with elevated viscosities, such as dielectric oils. Moreover, when considering the effect of buoyancy, the best performing HTF are deionised water and the two Cargill dielectric oils due to their high specific heat capacity and limited dynamic viscosity, i.e. high Rayleigh number.

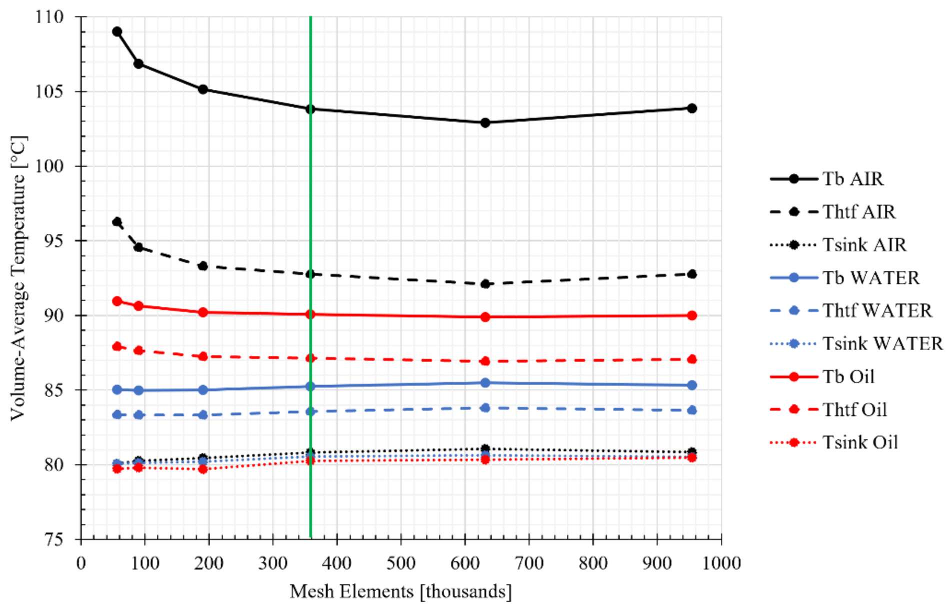

Figure 4: Mesh sensitivity analysis on volume-average temperatures of battery, HTF, and heat sink for three different HTF.

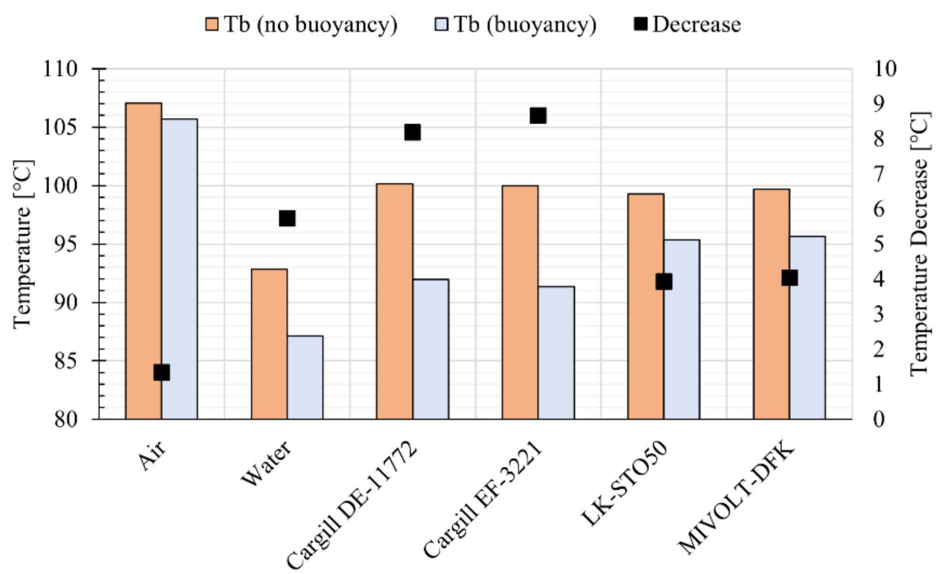

Figure 5: Steady-state average volume temperatures of battery: effect of buoyancy and HTF chemistry.

3.2. Effect of LIB volumetric heat generation rate

The effect of different LIB volumetric heat generation rates on the cooling performance of the TMS has been investigated using Cargill DE-11772 as the selected HTF. As expected, the volume average battery temperature increases mostly linearly with the heat generation rate. At low heat generation rates (1–25 kW/m³), the TMS ensures efficient cooling, with battery temperatures in the range of 27°C to 43°C, therefore limiting the need for convection to the heat sink (top) section of the TMS (refer to Figure 2.c). As the heat generation rates rises to high levels (75–100 kW/m³), the battery temperature rises to 91.13°C, pointing to the TMS cooling limitations, necessitating supplementary cooling techniques applied to both heat sink and lateral walls (refer to Figure 2, b and c) to sustain safe LIB operating conditions.

3.3. Effect of equivalent convective heat transfer coefficient on heat sink and insulation

Figure 6 illustrates the impact of varying the equivalent convective heat transfer coefficient of either the convection (heat sink) or insulation wall when using Cargill DE-11772 as HTF and under a volumetric heat generation rate of 100 kW/m³. It is evident that in this steady-state worst case scenario to guarantee operating temperatures below 60°C, the TMS should be exposed to 50 W/m² K at the heat sink (i.e. air force convection) or 15 W/m² K at the insulation wall (i.e. open-air natural convection). Overall, both enhanced heat sink and insulation properties are crucial for optimising thermal management and maintaining safe operating temperatures for the battery system.

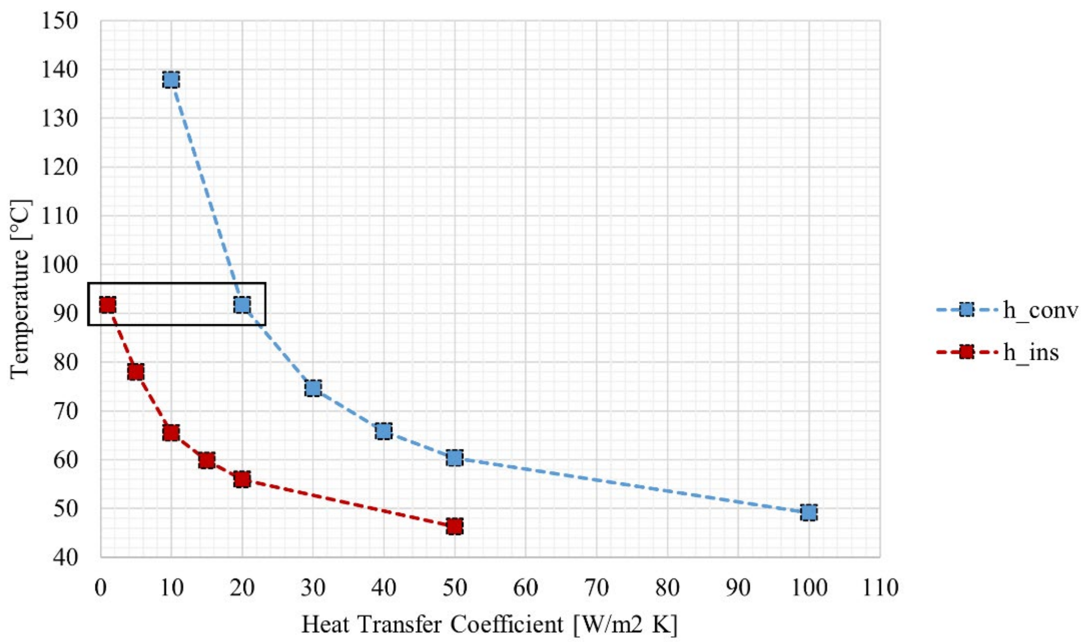

Figure 6: Effect of equivalent heat transfer coefficients on volume average battery temperature for convection wall (heat sink) and insulation wall, as defined in Figure 2. The dark square points to the benchmark values assumed in previous simulations, i.e. 20 W/m² K and 1 W/m² K for convection and insulation walls, respectively.

4. Conclusion

The study demonstrates the effectiveness of a hybrid thermal management system (TMS) combining heat pipes and dielectric fluid immersion cooling for LIB packs in light electric vehicles (LEVs). The hybrid system significantly outperforms conventional air cooling, reducing LIB temperatures and minimising thermal gradients, thereby preventing thermal hotspots and enhancing safety. The inclusion of buoyancy effects further improves cooling performance, especially for viscous dielectric fluids, reducing battery temperatures by up to 10°C.

At lower heat generation rates (1–50 kW/m³), the hybrid system maintains effective cooling, but as the rate increases to 100 kW/m³, the cooling capacity is challenged, with battery temperature reaching 91.13°C, indicating the need for supplementary cooling strategies under extreme conditions. Therefore, optimising the heat sink and insulation convective heat transfer coefficients is critical, as increasing these values significantly reduces LIB temperatures, highlighting the importance of sound TMS design.

Overall, the hybrid TMS, with its combination of heat pipes and immersion cooling, offers a promising solution for efficient and compact thermal management in LEVs, ensuring improved battery safety, performance, and lifespan under demanding operating conditions.

References

[1] S. Singh, S. Kumar, M. Vohra, S. Praveenkumar, D. Kumar, and S. Ghotekar, "An intense review on the performance of PCM-based lithium-ion battery cooling with aging effect in Indian climate conditions," *Inorganic Chemistry Communications,* vol. 169, 2024, doi: 10.1016/j.inoche.2024.113032.

[2] D. M. Weragoda, G. Tian, A. Burkitbayev, K.-H. Lo, and T. Zhang, "A comprehensive review on heat pipe based battery thermal management systems," *Applied Thermal Engineering,* vol. 224, 2023, doi: 10.1016/j.applthermaleng.2023.120070.

[3] A. Mitra, R. Kumar, D. K. Singh, and Z. Said, "Advances in the improvement of thermal-conductivity of phase change material-based lithium-ion battery thermal management systems: An updated review," *Journal of Energy Storage,* vol. 53, 2022, doi: 10.1016/j.est.2022.105195.

[4] W. Wu, G. F. Smaisim, S. M. Sajadi, M. A. Fagiry, Z. Li, M. A. Shamseldin, and H. Ş. Aybar, "Impact of phase change material-based heatsinks on lithium-ion battery thermal management: A comprehensive review," *Journal of Energy Storage,* vol. 52, 2022, doi: 10.1016/j.est.2022.104874.

[5] A. E. Misar and S. B. Thombre, "Thermal management of Li-ion battery pack using potting material and air cooling for electric two-wheelers," *Journal of Energy Storage,* vol. 101, 2024, doi: 10.1016/j.est.2024.113760.

[6] S.-b. Zhang, F. Nie, J.-p. Cheng, H. Yang, and Q. Gao, "Optimizing the air flow pattern to improve the performance of the air-cooling lithium-ion battery pack," *Applied Thermal Engineering,* vol. 236, 2024, doi: 10.1016/j.applthermaleng.2023.121486.

[7] M. Suresh Patil, J.-H. Seo, and M.-Y. Lee, "A novel dielectric fluid immersion cooling technology for Li-ion battery thermal management," *Energy Conversion and Management,* vol. 229, 2021, doi: 10.1016/j.enconman.2020.113715.

[8] X. Wu, Y. Lu, H. Ouyang, X. Ren, J. Yang, H. Guo, X. Han, C. Zhang, and Y. Wu, "Theoretical and experimental investigations on liquid immersion cooling battery packs for electric vehicles based on analysis of battery heat generation characteristics," *Energy Conversion and Management,* vol. 310, 2024, doi: 10.1016/j.enconman.2024.118478.

[9] J. Liu, Q. Ma, and X. Li, "Numerical study on heat dissipation performance of a lithium-ion battery module based on immersion cooling," *Journal of Energy Storage,* vol. 66, 2023, doi: 10.1016/j.est.2023.107511.

[10] A. Thiru Kumaran and S. Hemavathi, "Optimization of Lithium-ion battery thermal performance using dielectric fluid immersion cooling technique," *Process Safety and Environmental Protection,* vol. 189, pp. 768-781, 2024, doi: 10.1016/j.psep.2024.06.117.

[11] N. P. Williams, D. Trimble, and S. M. O'Shaughnessy, "An experimental investigation of liquid immersion cooling of a four cell lithium-ion battery module," *Journal of Energy Storage,* vol. 86, 2024, doi: 10.1016/j.est.2024.111289.

[12] Z. Zou, J. Xie, Y. Luo, G. Zhang, and X. Yang, "Numerical study on a novel thermal management system coupling immersion cooling with cooling tubes for power battery modules," *Journal of Energy Storage,* vol. 83, 2024, doi: 10.1016/j.est.2024.110634.

[13] Z. Wang, R. Zhao, S. Wang, and D. Huang, "Heat transfer characteristics and influencing factors of immersion coupled direct cooling for battery thermal management," *Journal of Energy Storage,* vol. 62, 2023, doi: 10.1016/j.est.2023.106821.

[14] Y. Wang, C. Li, X. Wen, W. Cai, Y. Jiang, C. Wen, Y. Wang, L. Hu, H. Yu, H. Zhu, H. Guo, and D. Liu, "Experimental studies on two-phase immersion liquid cooling for Li-ion battery thermal management," *Journal of Energy Storage,* vol. 72, 2023, doi: 10.1016/j.est.2023.108748.

[15] Q. Liu, C. Sun, J. Zhang, Q. Shi, K. Li, B. Yu, C. Xu, and X. Ju, "The electro-thermal equalization behaviors of battery modules with immersion cooling," *Applied Energy,* vol. 351, 2023, doi: 10.1016/j.apenergy.2023.121826.

[16] H. Zhu, Y. Ma, J. E, and S. Wei, "Channel structure design and optimization for immersion cooling system of lithium-ion batteries," *Journal of Energy Storage,* vol. 77, 2024, doi: 10.1016/j.est.2023.109930.